In revision

In vitro assessment of ATP-binding cassette transporters and their functional genetic polymorphisms on fluoroquinolone accumulation in human embryonic kidney 293 recombinant cell lines

Gwenaëlle Mahieu, Vincent Haufroid, Françoise Van Bambeke[+], Laure Elens[+]

[+]These authors share equal contribution as last authors

Pharmacologie cellulaire et moléculaire, Louvain Drug Research Institute (LDRI), Université catholique de Louvain (UCLouvain), Brussels, Belgium (M. G., F. V. B.) ; Integrated PharmacoMetrics, pharmacoGenomics and Pharmacokinetics (PMGK) Research group, Louvain Drug Research Institute (LDRI), Université catholique de Louvain (UCLouvain), Brussels, Belgium (M. G., L. E.) ; Louvain centre for Toxicology and Applied Pharmacology, Institut de recherche expérimentale et clinique (IREC), Université catholique de Louvain (UCLouvain), Brussels, Belgium (V. H., L. E.) ; Department of Clinical Chemistry, Cliniques Universitaires Saint-Luc, Brussels, Belgium (V. H.).

Running Title: Transporters and SNPs affecting fluoroquinolone disposition

Corresponding Author:

Françoise Van Bambeke, Prof.

Pharmacologie cellulaire et moléculaire, Louvain Drug Research Institute (LDRI)

Université catholique de Louvain (UCLouvain)

Avenue Emmanuel Mounier 73, B1.73.05

1200, Brussels, Belgium.

Tel: +32-2-764.73.78

e-mail: francoise.vanbambeke@uclouvain.be

Number of Text Pages: 20

Number of Tables: 0

Number of Figures: 6

Number of References: 55

Number of Words in Abstract: 249

Number of Words in Introduction: 627

Number of Words* in Discussion: 1505

* Word count without references

Non-standard Abbreviations

ABC, ATP-Binding Cassette; ABCB1, ATP-Binding Cassette subfamily B member 1; ABCC2,4, ATP-Binding Cassette subfamily C member 2, 4; ABCG2, ATP-Binding Cassette subfamily G member 2; ANOVA, Analysis Of Variance; BCRP, Breast Cancer Resistance Protein; CIP, Ciprofloxacin; Cmax, maximum plasma Concentration; FITC, Fluorescein isothiocyanate; HEK293, Human Embryonic Kidney 293; HRP, horseradish peroxidase; MAF, Minor Allele Frequency; MRP, Multidrug Resistance Protein; MRP4, Multidrug Resistance Protein 4; MXF, Moxifloxacin; Pg-p, P-glycoprotein; PheA, Pheophorbide A; qRT-PCR, quantitative Real-Time Polymerase Chain Reaction; Rh123, Rhodamine 123; SNP(s), Single Nucleotide Polymorphism(s); TBS-T, Tris-Buffered Saline with 0.02% Tween; WT, Wild Type.

Abstract

Fluoroquinolone tissue distribution and cellular accumulation are hindered by efflux transporters, including ABCB1, ABCG2, and ABCC4. Genetic polymorphisms (single nucleotide polymorphisms) can impact transporter activity, leading to interindividual variability in systemic and cellular pharmacokinetics of their substrates. This study assesses the impact of these transporters on moxifloxacin and ciprofloxacin cellular accumulation *in vitro,* and the effect of common single nucleotide polymorphisms in *ABCB1* (c.1199G>A (rs2229109); common haplotype c.1236C>T (rs1128503), c.2677G>T/A (rs2032582), and c.3435C>T (rs1045642)) and in *ABCG2* (c.421C>A (rs2231142)). Recombinant human embryonic kidney cell lines overexpressing wild type or variant transporters were generated via stable plasmid transfection. The impact of transporter overexpression on fluoroquinolone cell disposition was assessed through accumulation experiments in the presence of specific inhibitors to establish the link between transporter expression and differential accumulation. Results indicated that ABCB1 overexpression led to a 30% reduction in moxifloxacin and ciprofloxacin cellular concentrations, which was eliminated by zosuquidar or elacridar, while ABCG2 had no impact. ABCC4 markedly reduced ciprofloxacin accumulation by 25%, even at basal level, eliminated by MK517. Contrarily to the wild type and the c.1199A carriers, *ABCB1* CGT and TTT variants did not reduce antibiotic accumulation. In conclusion, moxifloxacin and ciprofloxacin are substrates of the wild type and 1199G>A ABCB1 and CGT and TTT haplotypes had a marginal impact on ABCB1 transport. Ciprofloxacin is a preferential ABCC4 substrate. Due to the large body distribution of these transporters, our findings may help rationalize their role and the impact of their polymorphisms in fluoroquinolone disposition in tissues and cells.

Significance Statement

This study demonstrates that moxifloxacin and ciprofloxacin are substrates of ABCB1, with ciprofloxacin also transported by ABCC4. Specific *ABCB1* polymorphisms (CGT and TTT haplotypes) reduce the ABCB1 transport capacity towards fluoroquinolones. These findings highlight the importance of considering ABCB1 and ABCC4 inducers or inhibitors, which may affect fluoroquinolone disposition in tissues and cells, as well as *ABCB1* polymorphisms that could explain interindividual variability in pharmacokinetic profiles.

1. Introduction

The fluoroquinolones moxifloxacin (MXF) and ciprofloxacin (CIP) are widely used in clinical practice due to their broad spectrum of activity, high bactericidal activity (Hooper, D. C., 2000; King et al., 2000; Van Bambeke et al., 2005), ability to accumulate in phagocytic and non-phagocytic cells (Easmon & Crane, 1985; Nix et al., 1991; Tulkens, 1991), and wide tissue distribution (Van Bambeke et al., 2005). As they can easily reach infection sites in various locations and accumulate therein, they exhibit useful activity against several intracellular bacteria thriving in different subcellular compartments (Barcia-Macay et al., 2006; Carlier et al., 1990; Carryn et al., 2002; Veziris et al., 2003).

However, this accumulation is controlled and possibly limited by efflux transporters that affect their body disposition and intracellular accumulation in infected cells, impacting their activity against intracellular bacteria (Marquez et al., 2009; Michot et al., 2004, 2005; Vallet et al., 2011; Van Bambeke, 2003). Transporter genes represent an important proportion of the human genome, as transporters exert vital roles in the bioavailability and cellular trafficking of endogenous and exogenous compounds. The ATP-binding cassette (ABC) superfamily is composed of 49 efflux transporters classified into seven subfamilies, designated A to G, based on their sequence homology (Choudhuri & Klaassen, 2006; Vasiliou et al., 2009). Located in the plasma membrane, these ATP-dependent active transporters unidirectionally translocate a wide range of substances (lipids, bile acids, xenobiotics, peptides) from the intracellular to the extracellular compartments (Choudhuri & Klaassen, 2006). By reducing the cellular concentration of potentially toxic compounds, they play a key role in body and tissue protection and detoxification (Fardel et al., 1996; Schinkel & Jonker, 2012).

Several lines of evidence indicate that certain efflux transporters may impact fluoroquinolone cellular accumulation. A potential role of ABCB1 (p-glycoprotein, P-gp) for MXF (Brillault et al., 2009, 2010) and CIP (Griffiths et al., 1993; Rodríguez-Ibáñez et al., 2003) and of ABCG2

(breast cancer resistance protein, BCRP) (Ando et al., 2007; Haslam et al., 2011) and ABCC4 (multidrug resistance protein 4, MRP4) (Haslam et al., 2011; Marquez et al., 2009; Michot et al., 2004, 2005) for CIP has been demonstrated. However, these data have been generated using different cell models or experimental procedures, rendering comparison difficult or impossible. Furthermore, these studies did not consider the potential influence of genetic polymorphisms.

In this study, we have evaluated the effect of these three ATP-binding cassette (ABC) transporters on moxifloxacin and CIP transport activity using comparable *in vitro* models of recombinant human embryonic kidney 293 (HEK293) cell lines. We also assessed the potential functional impact of the most common coding single nucleotide polymorphisms (SNPs) in ABCB1 and ABCG2. The *ABCB1* c.1199G>A coding SNP, located in exon 11 (rs2229109), has a reported minor allelic frequency (MAF) of around 6% in Caucasians and is associated with a serine to asparagine substitution at position 400 (Ser400Asn) in the sixth cytoplasmic loop of the ABCB1 transporter, a domain involved in substrate recognition (Dessilly et al., 2014). The three most common variants in the *ABCB1* coding region (rs1128503 (1236C>T, Gly412Gly), rs2032582 (2677G>T/A, Ala893Ser/Thr) and rs1045642 (3435C>T, Ile1145Ile)) are located in the sixth, tenth, and twelfth cytoplasmic loops, respectively. Among these, rs1128503 and rs1045642 are synonymous, while rs2032582 is nonsynonymous. These variants are commonly found in strong linkage disequilibrium, with a MAF of about 50% for the variant haplotype (TTT) in the Caucasian population (Choudhuri & Klaassen, 2006; Wolking et al., 2015). Lastly, the *ABCG2* c.421C>A coding SNP located in exon 5 (rs2231142) has a reported MAF of approximately 5-10% in Caucasians (Hira & Terada, 2018) and is associated with a glutamine-to-lysine substitution at position 141 (Gln141Lys) (Choudhuri & Klaassen, 2006) in the first cytoplasmic loop. Recent studies have associated this polymorphism with protein folding and trafficking default, partial degradation, and reduced overall and cell surface expression (Homolya, 2021).

2. Materials and methods

2.1 Drugs and chemicals

Moxifloxacin-HCl (MXF) and ciprofloxacin-HCl (CIP) were provided as microbiological standards by Bayer AG (Leverkusen, Germany); rhodamine 123 (Rh123), LY335979 (zosuquidar HCl), GF120918 (elacridar), MK571 NaCl, and Ko143 hydrate were obtained from Sigma-Aldrich (St-Louis, MO). Dulbecco's modified eagle medium, fetal bovine serum, penicillin/streptomycin (10,000 U mL^{-1}) and enzyme-free cell dissociation buffer were purchased from Gibco (Thermo Fisher Scientific, Waltham, MA); geneticin (G418) and hygromycin B were purchased from Roche (Basel, Switzerland), and pheophorbide a (PheA) was purchased from Sanbio (UDEN, The Netherlands). All flow cytometry antibodies (ABCB1 antibodies (Fluorescein isothiocyanate (FITC) mouse anti-human CD243, clone 17F9, reference 557002; and FITC mouse IgG2b κ isotype control, clone 27–35, reference 555742); ABCG2 antibodies (Peridinin Chlorophyll-Cyanine 5-5-a (PerCP-Cy^{TM}5.5) mouse anti-human CD338, reference 561460; and PerCP-Cy^{TM}5.5 mouse IgG2b κ isotype control, reference 558304)) were purchased from BD Biosciences (Franklin Lakes, NJ). All chemicals used in drug quantification were of analytical grade.

2.2 Cell lines and cell culture

All HEK293 cells were grown in Dulbecco's modified eagle medium with 4.5 g L^{-1} glucose, L-glutamine, and sodium pyruvate supplemented with 10% (v/v) of fetal bovine serum and 1% (v/v) of penicillin/streptomycin solution at a temperature of 37 °C in a 5% CO_2 atmosphere. For subculture, cells were detached using enzyme-free cell dissociation buffer.

HEK293 cells overexpressing the ABCC4 transporter were kindly supplied by Elaine M. Leslie from the University of Alberta (Canada) and selected in the presence of G418 (600 µg mL^{-1}) to select stable recombinant cells (Li et al., 2017).

2.3 Generation of ABCB1 recombinant cells

The generation of stable recombinant cell lines has been described previously (Dessilly et al., 2014, 2016b). In short, HEK293 cells were transfected with a pcDNA3.1 vector with cDNA encoding either the ABCB1 wild type (WT), variant, or an empty vector using Lipofectamine (Thermo Fisher Scientific). Stable recombinant cells were selected by incubating the transfected cells with G418 (1 mg mL^{-1}) 48 h after transfection. For $ABCB1_{1199G>A}$, three recombinant cell lines were generated: $HEK_{control}$ (pcDNA3.1 empty vector), HEK_{1199G} (wild type), and HEK_{1199A} (variant), and designated as CTL, 1199G, and 1199A in this study. For $ABCB1_{1236C>T - 2677G>T - 3435C>T}$, four cell lines were used: $HEK_{control}$, $HEK_{1236C-2677G-3435C}$ (wild type), and two different variant combinations, $HEK_{1236C-2677G-3435T}$ and $HEK_{1236T-2677T-3435T}$, referred to as CTL, CGC, CGT, and TTT respectively.

2.4 Generation of ABCG2 recombinant cells

HEK293 cells were transfected by Lipofectamine (Thermo Fisher Scientific) with a pCMV3 vector containing cDNA encoding either the ABCG2 WT (421C), the variant (421A), or a pCMV3 empty vector. Stable recombinant cells were selected by incubating the transfected cells with hygromycin B (0.5 mg mL^{-1}) 48 h after transfection. Three recombinant cell lines were generated, consisting of cell lines stably transfected with the pCMV3 empty vector ($HEK_{control}$), the WT vector (HEK_{421C}), or the variant vector (HEK_{421A}). These will be further referred to as CTL, 421C, and 421A.

2.4 Characterization of transfected cell lines

2.4.1 Characterization of transporter expression

2.4.1.1 Quantitative real-time polymerase chain reaction

Quantitative real-time polymerase chain reaction (qRT-PCR) was performed to quantify the number of *ABCB1*, *ABCG2*, *ABCC2*, and *ABCC4* gene copies in the different cell lines. Briefly,

RNA was extracted from cells (5×10^6 cells) using the RNeasy Mini Kit from Qiagen (Hilden, Germany) and reverse transcribed into cDNA following the GoScript Reverse Transcription Mix, Oligo(dT) Protocol (Promega, Madison, US) according to manufacturer instructions. qRT-PCR was carried out with SYBR-green (Bio-Rad, Hercules, CA) using the CFX96 Touch Real-Time PCR detection system (Bio-Rad). *18S* expression was used to normalize the expression of *ABCB1*, *ABCG2*, *ABCC2*, and *ABCC4*. The primer sequences for *18S*, *ABCB1*, *ABCG2*, *ABCC2*, and *ABCC4* were as follows: (forward) 5′-CGG CTA CCA CAT CCA AGG AA -3′ (reverse) 5′-ATA CGC TAT TGG AGC TGG AAT TAC C -3′ ; (forward) 5′-AGC AAA GGA GGC CAA CAT AC -3′ (reverse) 5′-GGC TTC ATC CAA AAG CAA AA -3′; (forward) 5'-CAG GAC TCA ATG CAA CAG GA-3' (reverse) 5'-TTC AGG TAG GCA ATT GTG AGG-3' ; (forward) 5'-CCT CAT TCA GAC GAC CAT CC-3' (reverse) 5'-ATT CTC AAT GCC AGC TTC CT-3' and (forward) 5'-AAA ATG TAC GCC TGG GAA AA-3' (reverse) 5'-GGT GAA GGT CAC AAA CAC GA-3'.

2.4.1.2 Western blot

The expression of transporter proteins was further characterized through western blot, according to a previously published method with certain modifications (Dessilly et al., 2014; Mahieu et al., 2024). Cell pellets were harvested using an adapted Radio ImmunoPrecipitation Assay lysis buffer (sodium deoxycholate 1%, tetraethylammonium bromide 100 mM, NaCl 300 mM, IGEPAL (Sigma-Aldrich) 2%, SDS 0.2%, n-dodecyl-β-D-maltoside 0.4%, pH 7.2-7.5) supplemented with a complete protease inhibitor cocktail (Roche) and incubated for 15 minutes on ice. Following this incubation, the cell lysates were then vortexed for 30 seconds and further diluted in LDS Sample Buffer (Invitrogen, Thermo Fisher Scientific) containing 25% of sample reducing agent (Invitrogen, Thermo Fischer Scientific) and water to achieve total protein concentrations of 12, 6, 3 µg for ABCB1; 10 µg for ABCG2 and ABCC4 in a final volume of 20 µL per sample. Each sample (20 µL) and 4 µL of protein ladder (PageRuler Prestained,

Thermo Fischer Scientific) were loaded onto a 4-12% Bis-Tris gel (NuPAGE, Thermo Fischer Scientific). The electrophoretic migration and the transfer of proteins onto a polyvinylidene difluoride transfer membrane (Thermo Fischer Scientific) were then achieved using a blotting pad (VWR, Leuven, Belgium) at an initial voltage of 175 V for 60 minutes followed by a reduced voltage of 30 V for 60 minutes. Blots were blocked with bovine serum albumin 1% in Tris-Buffered Saline with 0.02% Tween (TBS-T) pH 8 for at least 60 minutes. After three washing steps with Tris-Buffered Saline with 0.02% Tween (TBS-T) during 5 minutes, membranes were incubated overnight at 4°C with a monoclonal primary antibody depending on the targeting protein: anti-PgP (ab170904, rabbit, 1:10000 dilution, Abcam) for ABCB1; anti-MRP4 (ab233382, rabbit, 1:1000, Abcam) for ABCC4; anti-BCRP (ab207732, rabbit, 1:1000, Abcam) for ABCG2; and the monoclonal anti-β-Actin antibody (A1978, mouse, 1:2000 dilution, Sigma-Aldrich) for β-actin, diluted in Tris-Buffered Saline with 0.02% Tween (TBS-T) with milk powder (150 mg 5 mL^{-1} of TBS-T). The next day, after three steps of 5 minutes washing in TBS-T, membranes were incubated for 60 minutes with a secondary antibody diluted in TBS-T with milk powder (Anti-rabbit IgG horseradish peroxidase (HRP) (A27036, 1:2500 dilution, Invitrogen) for ABCB1 and ABCG2; Anti-Rabbit IgG H&L (HRP) (ab205718, 1/20 000 dilution, Abcam) for ABCC4; and Anti-mouse IgG (H+L) (A27025, 1:2500 dilution, Invitrogen) for β-Actin). Subsequently, after two additional 5-minutes washing steps in TBS-T and one washing step in Tris-Buffered Saline, protein detection was accomplished through chemiluminescence using HRP substrate (Immobilon Classico, Millipore, Burlington, MA).

2.4.1.3 Flow cytometry

ABCB1 and ABCG2 expression were evaluated after one week of growth in the presence of the selection antibiotics (G418 and Hygromycin B, respectively). The cell surface expression protein for ABCB1 and ABCG2 was evaluated by flow cytometry as previously described (Stillemans et al., 2021).

2.4.2 Characterization of transporter functionality using fluorescent substrates

For ABCB1, the functionality of the overexpressed transporter was assessed using the reference substrate Rh123 and two different ABCB1 inhibitors, namely zosuquidar (Alam et al., 2019; Dantzig et al., 2001; Dessilly et al., 2014) and elacridar (Dash et al., 2017), which differ by their mechanism of inhibition. Elacridar modulates ATPase activity, inhibiting ATP hydrolysis, essential for transporter activity (Dash et al., 2017). By contrast, zosuquidar directly docks in the substrate pocket of the transporter, blocking the change of conformation required for substrate efflux (Alam et al., 2019). The functionality of ABCG2 was assessed using PheA, a specific ABCG2 fluorescent substrate (Robey et al., 2004), and the ABCG2 inhibitor Ko143.

For these functional assays, 350,000 cells were plated in 12-well plates in complete medium one day before the experiment was performed. The next day, cells were incubated either for 120 minutes at 37 °C in a 5% CO_2 atmosphere in the dark with 5 µM Rh123 alone or in combination with either 0.2 µM zosuquidar or 5 µM elacridar, or for 60 minutes with 1 µM and 5 µM PheA alone or in combination with 1 µM Ko143. At the end of the incubation, the supernatants were discarded, the cells were washed twice with PBS at 4 °C, and lysed by adding 200 µL of water per well followed by overnight agitation in the dark at 4 °C. After 10 min of centrifugation at 14,000 rpm, the fluorescence of Rh123 and PheA in the supernatant were measured, using a Spectramax M3 fluorimeter (Molecular Devices, San José, CA) with excitation and emission wavelengths set at 485/530 nm and 410/600 nm, respectively.

2.5 Fluoroquinolone accumulation experiments

One day before the experiment, 350,000 cells were seeded in 12-well plates in 2 mL of complete medium. The next day, the medium was removed and replaced with fresh complete medium containing either MXF or CIP at 4 µg mL^{-1}, corresponding to the maximum plasma concentration (Cmax) observed in patients undergoing conventional therapy (Lettieri et al., 1992; Stass & Kubitza, 1999), alone or combined with ABCB1 inhibitors (zosuquidar 0.2 µM

or elacridar 5 µM), ABCG2 inhibitor (Ko143 1 µM), or a general Multidrug Resistance Protein (MRP) inhibitor (MK571 25 µM) to assess the role of ABCC4 (Tivnan et al., 2015). After 120 minutes of incubation at 37 °C in a 5% CO_2 atmosphere, the medium was discarded, cells were washed twice with PBS at 4 °C, and lysed by adding 200 µL of glycine-HCl buffer (pH 3) followed by overnight agitation in the dark at 4 °C. The next day, both cells and supernatant were transferred to a 1.5 mL Eppendorf (Hamburg, Germany) and centrifuged at 14,000 rpm for 10 minutes at 4 °C. Quantification of MXF and CIP was performed in the supernatant and proteins in the cell pellets for normalization.

2.6 Quantification of cell-associated fluoroquinolones

The cellular concentration of MXF and CIP were quantified by fluorometry using a Spectramax M3 fluorimeter with excitation and emission wavelengths set at 298/504 nm and at 275/450 nm, respectively (Michot et al., 2004, 2005). Calibration curves for both MXF and CIP were established within a concentration range of 10 ng mL^{-1} to 500 ng mL^{-1} and quantified in a similar fashion. For each experiment, the absolute amount of MXF and CIP recovered from the cell extracts were normalized to the amount of proteins measured using a DC (detergent compatible) Protein Assay from Bio-Rad (Hercules, CA) according to the manufacturer's instructions.

2.7 Statistics and data analysis

All accumulation data are mean ± standard error of the mean (SEM) expressed as a percentage of the CTL value (100%) of n experiments repeated at least three times (N = 3) in independent triplicates (n = 3 different wells), resulting in 9 independent values for statistical analysis. Statistical analysis was performed using GraphPad Prism version 8.0 (GraphPad software, San Diego, CA). Two-way analysis of variance (ANOVA) was performed under the null hypothesis

that the means of the groups compared were equal. When the differences between the means were significant ($P < 0.05$), Tukey's multiple comparison tests were performed.

3. Results

3.1 Characterization and validation of the recombinant models

Transporter expression

The expression of the different transporters of interest was quantified by qRT-PCR across all models, revealing marked increases in recombinant transporter transcripts compared to control cells (100-fold for *ABCB1* (Figure 1A), 1000-fold for *ABCG2* (Figure 1B), and 36-fold for *ABCC4* (Figure 1C)). At the protein level, western blot analysis showed stronger signals in recombinant models than in controls (Figures S1-S2-S3, supplemental data). Flow cytometry analysis of membrane transporter expression indicated that over 92% of the recombinant cell populations expressed the transporter, whereas control cells were negative for transporter expression (Figure S4, supplemental data). The expression of ABCC2, also described as a multidrug transporter, was similar and negligible (<0.1%) in all cell lines (Figure S5, supplemental data).

Transporter functionality

The functionality of ABCB1 and ABCG2 was evaluated by measuring their capacity to export specific fluorescent substrates, Rh123 and PheA, respectively. The results (Figure 2A, 2B) show significantly lower intracellular Rh123 fluorescence in cells overexpressing ABCB1 compared to control (CTL) cells, with a reduction of approximately four-fold ($P < 0.0009$) and, with no differences in Rh123 accumulation between WT (1199G, CGC) and variant (1199A, CGT, TTT) cell lines, indicating no impact of the studied polymorphisms on Rh123 accumulation. The addition of the specific ABCB1 inhibitor zosuquidar (Zo; Ki = 59 nM) (Dantzig et al., 2001) slightly increased the accumulation of Rh123 in control cells, which express a low but detectable basal level of *ABCB1* RNA transcripts (Figure 1A). Most evidently, both Zo and the non-specific ABCB1 inhibitor elacridar (Ela; Ki = 1.16 nM) (Kallem et al.,

2012) restored Rh123 cellular accumulation in ABCB1-transfected cells, bringing its concentration back to levels closer to those measured in the corresponding CTL cells.

Similar findings were obtained for the ABCG2 transporter and the PheA substrate. As shown in Figure 3, PheA fluorescence levels were lower in recombinant ABCG2 cells (421C, 421A) compared to control cells (CTL) at both tested concentrations, with a reduction of approximately 50% ($P < 0.0026$). The addition of the ABCG2 specific inhibitor Ko143 (Ki = 25.9 nM) ("Abstracts from the 10th European Regional ISSX Meeting," 2008; Zattoni et al., 2022) restored PheA cell-associated fluorescence in all recombinant cells. No effect of the 421C>A *ABCG2* polymorphism was observed at both PheA concentrations tested.

3.2 Effect of ABCB1 overexpression and polymorphisms on cellular fluoroquinolone concentrations

To evaluate the effect of transporters and inhibitors under clinically relevant conditions, experiments were conducted using fluoroquinolone concentrations corresponding to their Cmax.

3.2.1. 1199G>A polymorphism

A reduction of approximately 30% in the cellular concentration of MXF was observed in cell lines expressing either WT (1199G) or mutant (1199A) ABCB1, compared to the control (CTL) cells (Figure 4A1) ($P < 0.0040$). No significant difference was observed between cells expressing the WT or the variant protein. The addition of zosuquidar (Zo) or elacridar (Ela) abolished the effect of the overexpressed transporter, resulting in cellular concentrations similar to those observed in the CTL cell line, while Ko143 and the non-specific inhibitor MK571 (Kallem et al., 2012) were ineffective. In contrast, CIP showed the same level of accumulation in all cell lines, unaffected by Ko143, but significantly increased by MK571 in the CTL cell

line ($P < 0.0001$) or by zosuquidar and elacridar in both transfected cell lines (Figure 4A2) ($P < 0.0470$).

3.3.2. 1236C>T - 2677G>T - 3435C>T polymorphisms

Here also, the cellular concentration of MXF was significantly lower in the cell line overexpressing WT ABCB1 (CGC) compared to control cells (CTL) (Figure 4B1), showing a reduction of approximately 30% ($P < 0.0003$). Additionally, MXF concentration tended to be higher in CGT and TTT cells when compared to the WT haplotype (CGC) and no more different from that measured in CTL cells, suggesting that these two SNP haplotypes have a reduced effect on MXF transport. Regarding inhibitors, zosuquidar and, to a larger extent, elacridar increased MXF concentration in cells expressing the WT haplotype, but not significantly in cells expressing *ABCB1* polymorphisms. As observed in the experiments conducted with the 1199G>A polymorphism, Ko143 and MK571 had no significant effect on MXF cellular disposition in any cell line. Regarding CIP, its accumulation tended to be higher in cells overexpressing CGT or TTT variants than the WT transporter, reaching values similar to those measured in control cells. Elacridar, and to a lower extent zosuquidar, increased its accumulation in cells overexpressing the ABCB1 WT transporter or the CGT variant, but not the TTT variant (Figure 4B2). Here also, MK571 significantly increased CIP cellular disposition in CTL cells by approximately three-fold ($P < 0.0001$), while Ko143 had no effect on CIP disposition in any cell line.

3.5 Effect of ABCG2 overexpression and 421C>A polymorphism on cellular fluoroquinolone concentrations

Given that ABCG2 is known to facilitate the transport of CIP, we investigated the effect of ABCG2 overexpression and the impact of the 421C>A polymorphism on the cellular accumulation of MXF and CIP (Figure 5A, 5B). Both WT (421C) and variant (421A) ABCG2 cell lines showed similar cellular concentrations of MXF or CIP as compared to control cell

lines that express the transporter to a very low basal level (Figure 1B). Consistently, the addition of Ko143 had no effect on the MXF or CIP accumulation in any ABCG2 overexpressing cell lines. Furthermore, the addition of elacridar and of MK571 increased the accumulation of MXF and CIP, respectively, in CTL cell lines ($P < 0.0001$).

3.6 Effect of ABCC4 overexpression on cellular fluoroquinolone concentrations

To elucidate our observation that MK571 increases CIP accumulation in both CTL cell lines, we evaluated the impact of the ABCC4 transporter on MXF and CIP accumulation in a HEK293 recombinant model overexpressing ABCC4. The results presented in Figures 6A and 6B indicate that the ABCC4 transporter had no impact on MXF accumulation but significantly reduced that of CIP, with a reduction of approximately 25% ($P < 0.2222$). Furthermore, MK571 enhanced CIP accumulation in recombinant cells expressing ABCC4 and in CTL cells ($P < 0.0001$), consistent with our previous experiments. This effect of MK571 on CIP accumulation was concentration-dependent in recombinant cells but not in CTL cells.

4. Discussion

In this study, we assessed the functional relevance of ABCB1, ABCG2, and ABCC4 transporters and of key genetic polymorphisms in *ABCB1* and *ABCG2* (1199G>A; 1236C>T-2677G>T-3435C>T and 421C>A) for MXF and CIP cellular disposition. Stable HEK293 cell lines overexpressing WT (1199G and CGC for *ABCB1*; 421C for *ABCG2*) or variant alleles (1199A, CGT, and TTT for *ABCB1*; 421A for *ABCG2*) were generated.

To test the functionality of the overexpressed proteins, we analyzed the accumulation of the ABCB1 and ABCG2 substrates (Dessilly et al., 2014; Robey et al., 2004) and assessed the effects of specific inhibitors. We observed that Rh123 accumulation was four-fold lower in all ABCB1 transfected cell lines compared to CTL cells. These findings align with previous studies using the same cell model and further validate our experimental setting (Dessilly et al., 2014, 2016b). Furthermore, we demonstrate that Rh123 accumulation in CTL cells was slightly affected by the presence of the ABCB1 inhibitor zosuquidar (consistent with low ABCB1 basal expression in this model) and sensitive to both zosuquidar and elacridar in transfected cell lines. The concomitant use of the specific, competitive ABCB1 inhibitor zosuquidar (Dantzig et al., 2001) and of the non-specific, inhibiting ATP-hydrolysis, inhibitor elacridar enables more comprehensive ABCB1 inhibition by targeting different mechanisms (Alam et al., 2019; Dash et al., 2017). It allows comparison of their efficacy, assessment of interactions with *ABCB1* polymorphisms, and prevents compensatory drug efflux via other transporters like ABCG2, also inhibited by elacridar (Ki = 12.3 nM) ("Abstracts from the 10th European Regional ISSX Meeting," 2008).

For the ABCG2 transporter, a similar conclusion can be drawn as PheA accumulation was two-fold higher in CTL cells compared to those overexpressing ABCG2. Moreover, the ABCG2 specific inhibitor Ko143, which has no effect on PheA accumulation in CTL cells that express *ABCG2* to very low levels, restores it to CTL values in transfected cell lines.

Collectively, these experiments validate that both recombinant proteins (ABCB1 and ABCG2) and their variants are overexpressed, functional, and could be effectively inhibited by their respective inhibitors in this model.

Consistent with other *in vitro* studies (Brillault et al., 2009, 2010), our findings confirm the ABCB1 role in the active transport of MXF and, to a lesser extent, of CIP (Griffiths et al., 1993; Rodríguez-Ibáñez et al., 2003). ABCB1 transports various substrates that do not necessarily share structural similarities (Chufan et al., 2015), making it difficult to develop theories based on substrate structure only, even for drugs within the same pharmacological class. In this respect, it is worth mentioning that MXF is more lipophilic than CIP and essentially present in zwitterionic form at neutral pH (Michot et al., 2005). This might explain why MXF is better transported, as ABCB1 substrates are mainly hydrophobic and amphipathic compounds (Chufan et al., 2015).

Strikingly, we observe that the non-specific MRP transporter inhibitor MK571 (Ki < 2 µM) ("Abstracts from the 10th European Regional ISSX Meeting," 2008) increases by approximately three-fold in CIP accumulation in all CTL clones. This effect may be due to ABCC4 basal expression in these cells. Confirming this hypothesis, and in accordance with previous observations in J774 macrophages overexpressing ABCC4 (Marquez et al., 2009; Michot et al., 2006), CIP accumulation is reduced by approximately 25% in HEK cells overexpressing ABCC4, and higher MK571 concentrations (50 µM) are needed to restore CIP accumulation in these cells. Consequently, our hypothesis is that ABCC4 basal expression in all HEK293 cell lines reduces CIP accumulation and, hence, the expected role of ABCB1 and ABCG2 (Ando et al., 2007) in transfected cells. These results highlight the importance of carefully considering the basal expression of transporters in a given cell line, as they can have a non-negligible impact on drug substrate accumulation, leading to erroneous interpretation of the overexpressed transporter's real impact in the same cell line. In the present case, the effects of non-specific,

and to a lesser extent, specific ABCB1 inhibitors remains observable in cells overexpressing ABCB1 or its variants, but it might have been different in cells that did not express ABCC4 and accumulated more CIP.

Lastly, we did not find any significant effect of ABCG2 or its genetic polymorphisms on CIP and MXF cellular accumulation. To the best of our knowledge, MXF transport by ABCG2 has not been reported so far, and its role in CIP transport does not seem predominant in the presence of other efflux transporters (Ando et al., 2007; Haslam et al., 2011).

We did not detect any significant effect of certain SNPs investigated. Specifically, MXF or CIP cellular accumulation in cells overexpressing *ABCB1* 1199A or *ABCG2* 421A variant alleles did not differ from that measured in cells overexpressing the corresponding WT transporter. Previous studies have demonstrated that the 1199G>A SNP influences the transporter activity in a substrate-dependent manner. For instance, the 1199A variant exhibited reduced ABCB1 activity towards tacrolimus in recombinant HEK293 and K512 cell lines, while it enhanced ABCB1 activity towards vinblastine in K562 recombinant cell lines (Dessilly et al., 2014). However, this variant did not significantly affect cyclosporin A, Rh123 (HEK293 and K562), doxorubicin (K562), or rivaroxaban (HEK293) (Sennesael et al., 2018), darunavir (HEK293) (Stillemans et al., 2021) or bictegravir (HEK293) transport (De Greef et al., 2024). Similarly, the *in vitro* effect of the 1199G>A SNP was less pronounced for nilotinib compared to imatinib (HEK293), a better ABCB1 substrate (Dessilly et al., 2016a). Given its localization in the sixth cytoplasmic loop involved in substrate recognition, the 1199G>A polymorphism may selectively influence the binding of certain substrates while leaving others unaffected. Two distinct binding sites have been identified in ABCB1, namely H- and R-sites. H-site is involved in highly hydrophobic substrate recognition, while R-site recognizes smaller substrates and facilitates ATP hydrolysis, both essential for ABCB1 transport (Ferreira et al., 2013). At the present time, however, it is unknown if 1199G>A *ABCB1* polymorphism might impact

substrate interaction with these sites and in which site MXF or other substrates bind in this pocket, making it difficult to rationalize how it may affect various drugs (Chufan et al., 2013). In contrast to the WT ABCB1 protein, the TTT and CGT haplotypes either do not, or only minimally reduce the cellular accumulation of MXF and CIP. Both haplotypes share the variant at the third nucleotide (c.3435C>T), suggesting its possible causative role. To our knowledge, this is the first *in vitro* study that has investigated the role of these polymorphisms on fluoroquinolone disposition. Limited *in vivo* studies have shown specific impact on fluoroquinolone pharmacokinetics. For example, the *ABCB1* 3435C>T (CGT) polymorphism is associated with a decrease in the sitafloxacin Cmax (Sun et al., 2021). It introduces a rare codon that causes a ribosome translational pause, which affects protein folding kinetics by chaperones, thereby altering ABCB1 function (Kimchi-Sarfaty et al., 2007). Additionally, the *ABCB1* 2677T>G/A (rs2032582) polymorphism correlates with a 40% reduction in MXF prehepatic bioavailability in humans, leading to a decrease in the area under the curve (Naidoo et al., 2018). These data suggest that the reduced function of this variant increases fluoroquinolone cellular and tissue distribution, supported by our *in vitro* data, which further identifies the c.3435C>T SNP within the haplotype as the causative variant.

As for the TTT variant haplotype, although there is ongoing debate about the functional implications of this haplotype, literature indicates a trend towards higher drug blood concentrations associated with these SNPs. For example, the *ABCB1* TTT variant haplotype is linked to increased accumulation of imatinib compared to *ABCB1* CGC (Dessilly et al., 2016b), also in line with our own findings with MXF and CIP.

In summary, ABCB1, which is predominantly expressed in epithelial cells, plays a pivotal role in the absorption, distribution, and excretion of various substrates, including antibiotics. This study has demonstrated that this transporter significantly influences fluoroquinolone cellular concentration *in vitro*, with a more pronounced effect on MXF than on CIP and highlights the

impact of specific polymorphisms. These findings may help explain the limited *in vivo* data suggesting that ABCB1 genetic polymorphisms can affect fluoroquinolone disposition. Noteworthy, the 3435TT genotype is more common in white populations, while the CC genotype is more frequent in Africans (Schaeffeler et al., 2001), indicating the potential value of comparing fluoroquinolone pharmacokinetics in these populations.

Conversely, ABCC4, expressed in phagocytic cells (Marquez et al., 2009), reduces by approximately 25% the intracellular CIP concentration, potentially impacting its efficacy against intracellular pathogens (Lismond et al., 2008). The consequences of these modulations need to be addressed in terms of efficacy, risks of resistance selection, or toxicity in well-designed *in vivo* or clinical studies.

Despite these important findings, some limitations of this work should be acknowledged. Indeed, using a cell model overexpressing a specific transporter may not accurately reflect its role in the body, where its expression could be lower, and multiple transporters may interact to modulate drug disposition. However, these models remain valuable in pharmacology for understanding substrate specificity and comparing the impact of genetic polymorphisms. A model incorporating all relevant transporters may nevertheless usefully complement this work to assess the individual contribution and relative importance of each transporter in MXF and CIP disposition. Secondly, only key polymorphisms of *ABCB1* and *ABCG2* were explored, but the study would need to be extended to others in the future. Lastly, the *in vitro* nature of the study does not capture the complexity of pharmacokinetic processes like tissue distribution or hepatic or renal elimination which involve transporters *in vivo*. Nevertheless, our work may help understanding interindividual variations in fluoroquinolone pharmacokinetics among patients.

To conclude, in HEK293 recombinant cell models, our study indicates that ABCB1 plays a significant role in MXF transport, while ABCC4 is more crucial for CIP transport. Additionally, we show that *ABCB1* CGT and TTT haplotypes seem to reduce ABCB1 efflux ability towards these compounds. Importantly also, our work highlights the need to consider the interfering role of the basal expression of transporters when studying drug transport in recombinant cell lines to correctly interpret the resulting data.

Acknowledgements

The authors thank Nadtha Panin, Maxime Lingursky and Virginie Mohymont for technical support for cell culture and specific experiments. The authors also thank Elaine M. Leslie for kindly providing HEK293 cells overexpressing the ABCC4 transporter.

Authorship contribution

Participated in research design: G. M., F. V. B. and L. E.

Conducted experiments: G. M.

Contributed new reagents or analytic tools: V. H.

Performed data analysis: G. M. and F. V. B.

Wrote and contributed to the writing of the manuscript: G. M., V. H., F. V. B. and L. E.

References

Abstracts from the 10 th European Regional ISSX Meeting. (2008). *Drug Metabolism Reviews*, *40*(sup1), 1–172. https://doi.org/10.1080/03602530801949332

Alam, A., Kowal, J., Broude, E., Roninson, I., & Locher, K. P. (2019). Structural insight into substrate and inhibitor discrimination by human P-glycoprotein. *Science*, *363*(6428), 753–756. https://doi.org/10.1126/science.aav7102

Ando, T., Kusuhara, H., Merino, G., Alvarez, A. I., Schinkel, A. H., & Sugiyama, Y. (2007). Involvement of Breast Cancer Resistance Protein (*ABCG2*) in the Biliary Excretion Mechanism of Fluoroquinolones. *Drug Metabolism and Disposition*, *35*(10), 1873–1879. https://doi.org/10.1124/dmd.107.014969

Barcia-Macay, M., Seral, C., Mingeot-Leclercq, M.-P., Tulkens, P. M., & Van Bambeke, F. (2006). Pharmacodynamic Evaluation of the Intracellular Activities of Antibiotics against *Staphylococcus aureus* in a Model of THP-1 Macrophages. *Antimicrobial Agents and Chemotherapy*, *50*(3), 841–851. https://doi.org/10.1128/AAC.50.3.841-851.2006

Brillault, J., De Castro, W. V., & Couet, W. (2010). Relative Contributions of Active Mediated Transport and Passive Diffusion of Fluoroquinolones with Various Lipophilicities in a Calu-3 Lung Epithelial Cell Model. *Antimicrobial Agents and Chemotherapy*, *54*(1), 543–545. https://doi.org/10.1128/AAC.00733-09

Brillault, J., De Castro, W. V., Harnois, T., Kitzis, A., Olivier, J.-C., & Couet, W. (2009). P-Glycoprotein-Mediated Transport of Moxifloxacin in a Calu-3 Lung Epithelial Cell Model. *Antimicrobial Agents and Chemotherapy*, *53*(4), 1457–1462. https://doi.org/10.1128/AAC.01253-08

Carlier, M. B., Scorneaux, B., Zenebergh, A., Desnottes, J. F., & Tulkens, P. M. (1990). Cellular uptake, localization and activity of fluoroquinolones in uninfected and infected macrophages. *The Journal of Antimicrobial Chemotherapy*, *26 Suppl B*, 27–39. https://doi.org/10.1093/jac/26.suppl_b.27

Carryn, S., Van Bambeke, F., Mingeot-Leclercq, M.-P., & Tulkens, P. M. (2002). Comparative Intracellular (THP-1 Macrophage) and Extracellular Activities of β-Lactams, Azithromycin, Gentamicin, and Fluoroquinolones against *Listeria monocytogenes* at Clinically Relevant Concentrations. *Antimicrobial Agents and Chemotherapy*, *46*(7), 2095–2103. https://doi.org/10.1128/AAC.46.7.2095-2103.2002

Choudhuri, S., & Klaassen, C. D. (2006). Structure, Function, Expression, Genomic Organization, and Single Nucleotide Polymorphisms of Human ABCB1 (MDR1), ABCC (MRP), and ABCG2 (BCRP) Efflux Transporters. *International Journal of Toxicology*, *25*(4), 231–259. https://doi.org/10.1080/10915810600746023

Chufan, E. E., Kapoor, K., Sim, H.-M., Singh, S., Talele, T. T., Durell, S. R., & Ambudkar, S. V. (2013). Multiple Transport-Active Binding Sites Are Available for a Single Substrate on Human P-Glycoprotein (ABCB1). *PLoS ONE*, *8*(12), e82463. https://doi.org/10.1371/journal.pone.0082463

Chufan, E. E., Sim, H.-M., & Ambudkar, S. V. (2015). Molecular Basis of the Polyspecificity of P-Glycoprotein (ABCB1). In *Advances in Cancer Research* (Vol. 125, pp. 71–96). Elsevier. https://doi.org/10.1016/bs.acr.2014.10.003

Dantzig, A., Law, K., Cao, J., & Starling, J. (2001). Reversal of Multidrug Resistance by the P-Glycoprotein Modulator, LY335979, from the Bench to the Clinic. *Current Medicinal Chemistry*, *8*(1), 39–50. https://doi.org/10.2174/0929867013373903

Dash, R. P., Jayachandra Babu, R., & Srinivas, N. R. (2017). Therapeutic Potential and Utility of Elacridar with Respect to P-glycoprotein Inhibition: An Insight from the Published In Vitro, Preclinical and Clinical Studies. *European Journal of Drug Metabolism and Pharmacokinetics*, *42*(6), 915–933. https://doi.org/10.1007/s13318-017-0411-4

De Greef, J., Akue, M., Panin, N., Delongie, K.-A., André, M., Mahieu, G., Hoste, E., Elens, L., Belkhir, L., & Haufroid, V. (2024). Effect of ABCB1 most frequent polymorphisms on the accumulation of bictegravir in recombinant HEK293 cell lines. *Scientific Reports*, *14*(1), 16290. https://doi.org/10.1038/s41598-024-66809-0

554 Dessilly, G., Elens, L., Panin, N., Capron, A., Decottignies, A., Demoulin, J.-B., & Haufroid, V. (2014).
555 ABCB1 1199G>A genetic polymorphism (Rs2229109) influences the intracellular
556 accumulation of tacrolimus in HEK293 and K562 recombinant cell lines. *PloS One*, *9*(3),
557 e91555. https://doi.org/10.1371/journal.pone.0091555
558 Dessilly, G., Elens, L., Panin, N., Karmani, L., Demoulin, J.-B., & Haufroid, V. (2016a). *ABCB1*
559 1199G>A Polymorphism (rs2229109) Affects the Transport of Imatinib, Nilotinib and
560 Dasatinib. *Pharmacogenomics*, *17*(8), 883–890. https://doi.org/10.2217/pgs-2016-0012
561 Dessilly, G., Panin, N., Elens, L., Haufroid, V., & Demoulin, J.-B. (2016b). Impact of ABCB1
562 1236C > T-2677G > T-3435C > T polymorphisms on the anti-proliferative activity of imatinib,
563 nilotinib, dasatinib and ponatinib. *Scientific Reports*, *6*, 29559.
564 https://doi.org/10.1038/srep29559
565 Easmon, C. S., & Crane, J. P. (1985). Uptake of ciprofloxacin by macrophages. *Journal of Clinical*
566 *Pathology*, *38*(4), 442–444. https://doi.org/10.1136/jcp.38.4.442
567 Fardel, O., Lecureur, V., & Guillouzo, A. (1996). The P-glycoprotein multidrug transporter. *General*
568 *Pharmacology: The Vascular System*, *27*(8), 1283–1291. https://doi.org/10.1016/S0306-
569 3623(96)00081-X
570 Ferreira, R. J., Ferreira, M.-J. U., & Dos Santos, D. J. V. A. (2013). Molecular Docking Characterizes
571 Substrate-Binding Sites and Efflux Modulation Mechanisms within P-Glycoprotein. *Journal of*
572 *Chemical Information and Modeling*, *53*(7), 1747–1760. https://doi.org/10.1021/ci400195v
573 Griffiths, N. M., Hirst, B. H., & Simmons, N. L. (1993). Active secretion of the fluoroquinolone
574 ciprofloxacin by human intestinal epithelial Caco-2 cell layers. *British Journal of*
575 *Pharmacology*, *108*(3), 575–576. https://doi.org/10.1111/j.1476-5381.1993.tb12844.x
576 Haslam, I. S., Wright, J. A., O'Reilly, D. A., Sherlock, D. J., Coleman, T., & Simmons, N. L. (2011).
577 Intestinal Ciprofloxacin Efflux: The Role of Breast Cancer Resistance Protein (ABCG2). *Drug*
578 *Metabolism and Disposition*, *39*(12), 2321–2328. https://doi.org/10.1124/dmd.111.038323
579 Hira, D., & Terada, T. (2018). BCRP/ABCG2 and high-alert medications: Biochemical,
580 pharmacokinetic, pharmacogenetic, and clinical implications. *Biochemical Pharmacology*, *147*,
581 201–210. https://doi.org/10.1016/j.bcp.2017.10.004

582 Homolya, L. (2021). Medically Important Alterations in Transport Function and Trafficking of ABCG2.
583 *International Journal of Molecular Sciences*, *22*(6), 2786.
584 https://doi.org/10.3390/ijms22062786
585 Hooper, D. C. (2000). *Fluoroquinolones*. 404–423.
586 Kallem, R., Kulkarni, C. P., Patel, D., Thakur, M., Sinz, M., Singh, S. P., Mahammad, S. S., &
587 Mandlekar, S. (2012). A simplified protocol employing elacridar in rodents: A screening model
588 in drug discovery to assess P-gp mediated efflux at the blood brain barrier. *Drug Metabolism*
589 *Letters*, *6*(2), 134–144.
590 Kimchi-Sarfaty, C., Oh, J. M., Kim, I.-W., Sauna, Z. E., Calcagno, A. M., Ambudkar, S. V., &
591 Gottesman, M. M. (2007). A "silent" polymorphism in the MDR1 gene changes substrate
592 specificity. *Science (New York, N.Y.)*, *315*(5811), 525–528.
593 https://doi.org/10.1126/science.1135308
594 King, D. E., Malone, R., & Lilley, S. H. (2000). New classification and update on the quinolone
595 antibiotics. *American Family Physician*, *61*(9), 2741–2748.
596 Lettieri, J. T., Rogge, M. C., Kaiser, L., Echols, R. M., & Heller, A. H. (1992). Pharmacokinetic profiles
597 of ciprofloxacin after single intravenous and oral doses. *Antimicrobial Agents and*
598 *Chemotherapy*, *36*(5), 993–996. https://doi.org/10.1128/AAC.36.5.993
599 Li, J., Bauer, M., Moe, B., Leslie, E. M., & Li, X.-F. (2017). Multidrug Resistance Protein 4
600 (MRP4/ABCC4) Protects Cells from the Toxic Effects of Halobenzoquinones. *Chemical*
601 *Research in Toxicology*, *30*(10), 1815–1822. https://doi.org/10.1021/acs.chemrestox.7b00156
602 Lismond, A., Tulkens, P. M., Mingeot-Leclercq, M.-P., Courvalin, P., & Van Bambeke, F. (2008).
603 Cooperation between prokaryotic (Lde) and eukaryotic (MRP) efflux transporters in J774
604 macrophages infected with Listeria monocytogenes: Studies with ciprofloxacin and
605 moxifloxacin. *Antimicrobial Agents and Chemotherapy*, *52*(9), 3040–3046.
606 https://doi.org/10.1128/AAC.00105-08
607 Mahieu, G., Sennesael, A.-L., Pochet, L., Haufroid, V., Van Bambeke, F., Spinewine, A., & Elens, L.
608 (2024). In vitro assessment of the risk of ABCB1-mediated drug–drug interaction between
609 rivaroxaban and tacrolimus in human embryonic kidney 293 recombinant cell lines. *Research*

and Practice in Thrombosis and Haemostasis, *8*(5), 102521. https://doi.org/10.1016/j.rpth.2024.102521

Marquez, B., Caceres, N. E., Mingeot-Leclercq, M.-P., Tulkens, P. M., & Van Bambeke, F. (2009). Identification of the efflux transporter of the fluoroquinolone antibiotic ciprofloxacin in murine macrophages: Studies with ciprofloxacin-resistant cells. *Antimicrobial Agents and Chemotherapy*, *53*(6), 2410–2416. https://doi.org/10.1128/AAC.01428-08

Michot, J.-M., Heremans, M. F., Caceres, N. E., Mingeot-Leclercq, M.-P., Tulkens, P. M., & Van Bambeke, F. (2006). Cellular Accumulation and Activity of Quinolones in Ciprofloxacin-Resistant J774 Macrophages. *Antimicrobial Agents and Chemotherapy*, *50*(5), 1689–1695. https://doi.org/10.1128/AAC.50.5.1689-1695.2006

Michot, J.-M., Seral, C., Van Bambeke, F., Mingeot-Leclercq, M.-P., & Tulkens, P. M. (2005). Influence of efflux transporters on the accumulation and efflux of four quinolones (ciprofloxacin, levofloxacin, garenoxacin, and moxifloxacin) in J774 macrophages. *Antimicrobial Agents and Chemotherapy*, *49*(6), 2429–2437. https://doi.org/10.1128/AAC.49.6.2429-2437.2005

Michot, J.-M., Van Bambeke, F., Mingeot-Leclercq, M.-P., & Tulkens, P. M. (2004). Active efflux of ciprofloxacin from J774 macrophages through an MRP-like transporter. *Antimicrobial Agents and Chemotherapy*, *48*(7), 2673–2682. https://doi.org/10.1128/AAC.48.7.2673-2682.2004

Naidoo, A., Ramsuran, V., Chirehwa, M., Denti, P., McIlleron, H., Naidoo, K., Yende-Zuma, N., Singh, R., Ngcapu, S., Chaudhry, M., Pepper, M. S., & Padayatchi, N. (2018). Effect of genetic variation in UGT1A and ABCB1 on moxifloxacin pharmacokinetics in South African patients with tuberculosis. *Pharmacogenomics*, *19*(1), 17–29. https://doi.org/10.2217/pgs-2017-0144

Nix, D. E., Goodwin, S. D., Peloquin, C. A., Rotella, D. L., & Schentag, J. J. (1991). Antibiotic tissue penetration and its relevance: Models of tissue penetration and their meaning. *Antimicrobial Agents and Chemotherapy*, *35*(10), 1947–1952. https://doi.org/10.1128/AAC.35.10.1947

Robey, R. W., Steadman, K., Polgar, O., Morisaki, K., Blayney, M., Mistry, P., & Bates, S. E. (2004). Pheophorbide a Is a Specific Probe for ABCG2 Function and Inhibition. *Cancer Research*, *64*(4), 1242–1246. https://doi.org/10.1158/0008-5472.CAN-03-3298

Rodríguez-Ibáñez, M., Nalda-Molina, R., Montalar-Montero, M., Bermejo, M. V., Merino, V., & Garrigues, T. M. (2003). Transintestinal secretion of ciprofloxacin, grepafloxacin and sparfloxacin: In vitro and in situ inhibition studies. *European Journal of Pharmaceutics and Biopharmaceutics*, *55*(2), 241–246. https://doi.org/10.1016/S0939-6411(02)00185-6

Schaeffeler, E., Eichelbaum, M., Brinkmann, U., Penger, A., Asante-Poku, S., Zanger, U. M., & Schwab, M. (2001). Frequency of C3435T polymorphism of MDR1 gene in African people. *The Lancet*, *358*(9279), 383–384. https://doi.org/10.1016/S0140-6736(01)05579-9

Schinkel, A. H., & Jonker, J. W. (2012). Mammalian drug efflux transporters of the ATP binding cassette (ABC) family: An overview. *Advanced Drug Delivery Reviews*, *64*, 138–153. https://doi.org/10.1016/j.addr.2012.09.027

Sennesael, A.-L., Panin, N., Vancraeynest, C., Pochet, L., Spinewine, A., Haufroid, V., & Elens, L. (2018). Effect of ABCB1 genetic polymorphisms on the transport of rivaroxaban in HEK293 recombinant cell lines. *Scientific Reports*, *8*(1), 10514. https://doi.org/10.1038/s41598-018-28622-4

Stass, H., & Kubitza, D. (1999). Pharmacokinetics and elimination of moxifloxacin after oral and intravenous administration in man. *Journal of Antimicrobial Chemotherapy*, *43*(suppl_2), 83–90. https://doi.org/10.1093/jac/43.suppl_2.83

Stillemans, G., Djokoto, H. P., Delongie, K.-A., El-Hamdaoui, H., Panin, N., Haufroid, V., & Elens, L. (2021). Effect of four ABCB1 genetic polymorphisms on the accumulation of darunavir in HEK293 recombinant cell lines. *Scientific Reports*, *11*(1), 9000. https://doi.org/10.1038/s41598-021-88365-7

Sun, L., Sun, G., Yang, Y., Shen, Y., Huang, F., Xie, L., Cheng, J., Zhang, H., Zhang, X., Liu, Y., & Wang, Y. (2021). Effects of *ABCB1* , *UGT1A1* , and *UGT1A9* Genetic Polymorphisms on the Pharmacokinetics of Sitafloxacin Granules in Healthy Subjects. *Clinical Pharmacology in Drug Development*, *10*(1), 57–67. https://doi.org/10.1002/cpdd.848

Tivnan, A., Zakaria, Z., O'Leary, C., Kögel, D., Pokorny, J. L., Sarkaria, J. N., & Prehn, J. H. M. (2015). Inhibition of multidrug resistance protein 1 (MRP1) improves chemotherapy drug response in

primary and recurrent glioblastoma multiforme. *Frontiers in Neuroscience*, *9*, 218. https://doi.org/10.3389/fnins.2015.00218

Tulkens, P. M. (1991). Intracellular distribution and activity of antibiotics. *European Journal of Clinical Microbiology & Infectious Diseases: Official Publication of the European Society of Clinical Microbiology*, *10*(2), 100–106. https://doi.org/10.1007/BF01964420

Vallet, C. M., Marquez, B., Nhiri, N., Anantharajah, A., Mingeot-Leclercq, M.-P., Tulkens, P. M., Lallemand, J.-Y., Jacquet, E., & Van Bambeke, F. (2011). Modulation of the expression of ABC transporters in murine (J774) macrophages exposed to large concentrations of the fluoroquinolone antibiotic moxifloxacin. *Toxicology*, *290*(2–3), 178–186. https://doi.org/10.1016/j.tox.2011.09.003

Van Bambeke, F. (2003). Antibiotic efflux pumps in eukaryotic cells: Occurrence and impact on antibiotic cellular pharmacokinetics, pharmacodynamics and toxicodynamics. *Journal of Antimicrobial Chemotherapy*, *51*(5), 1067–1077. https://doi.org/10.1093/jac/dkg225

Van Bambeke, F., Michot, J.-M., Van Eldere, J., & Tulkens, P. M. (2005). Quinolones in 2005: An update. *Clinical Microbiology and Infection*, *11*(4), 256–280. https://doi.org/10.1111/j.1469-0691.2005.01131.x

Vasiliou, V., Vasiliou, K., & Nebert, D. W. (2009). Human ATP-binding cassette (ABC) transporter family. *Human Genomics*, *3*(3), 281–290. https://doi.org/10.1186/1479-7364-3-3-281

Veziris, N., Truffot-Pernot, C., Aubry, A., Jarlier, V., & Lounis, N. (2003). Fluoroquinolone-containing third-line regimen against Mycobacterium tuberculosis in vivo. *Antimicrobial Agents and Chemotherapy*, *47*(10), 3117–3122. https://doi.org/10.1128/AAC.47.10.3117-3122.2003

Wolking, S., Schaeffeler, E., Lerche, H., Schwab, M., & Nies, A. T. (2015). Impact of Genetic Polymorphisms of ABCB1 (MDR1, P-Glycoprotein) on Drug Disposition and Potential Clinical Implications: Update of the Literature. *Clinical Pharmacokinetics*, *54*(7), 709–735. https://doi.org/10.1007/s40262-015-0267-1

Zattoni, I. F., Delabio, L. C., Dutra, J. D. P., Kita, D. H., Scheiffer, G., Hembecker, M., Pereira, G. D. S., Moure, V. R., & Valdameri, G. (2022). Targeting breast cancer resistance protein

692 (BCRP/ABCG2): Functional inhibitors and expression modulators. *European Journal of*
693 *Medicinal Chemistry*, *237*, 114346. https://doi.org/10.1016/j.ejmech.2022.114346
694

Dataset/Data Availability Statement

The data that support the findings of this study are available from the corresponding author upon reasonable request.

Footnote

G.M. is a research fellow (FC43775), and F.V.B. is a research director from the Belgian Fonds de la Recherche Scientifique (FRS-FNRS).

This work was supported by the Belgian Fonds de la Recherche Scientifique [GRANT T.0205.22] to F. V. B.

The authors declare no conflict of interest.

Figure Legends

Figure 1. ABC transporter RNA transcripts. ABC transporter RNA expression levels normalized to the *18S* expression level (housekeeping gene) in (**A)** $HEK_{control}$ (CTL), $HEK_{1199G>A}$ (1199G, 1199A) and $HEK_{1236C>T\text{-}2677G>T\text{-}3435C>T}$ (CGC, CGT, TTT) cell lines; (**B)** $HEK_{control}$ (CTL) and $HEK_{421C>A}$ (421C, 421A) cell lines; (**C)** $HEK_{control}$ (CTL) and HEK_{ABCC4} (ABCC4) cell lines. The $HEK_{control}$ (CTL) in each panel corresponds to the clone used to overexpress the corresponding transporter and transfected by the corresponding empty vector. Results are reported as mean ± SD (n = 3). Statistical analysis: 2-way ANOVA with Tukey post-hoc test, comparison between all transporters in all cell lines. Values with different letters are statistically different from each other ($P < 0.05$).

Figure 2. Impact of ABCB1 transporter on the cellular accumulation of rhodamine 123 (Rh123). Cell-associated fluorescence of Rh123 (5 µM) after 2 h of incubation in control conditions or in the presence of the ABCB1 inhibitors zosuquidar (Zo; 0.2 µM) or elacridar (Ela; 5 µM) in **(A)** $HEK_{control}$ (CTL), $HEK_{wild\ type}$ (1199G), $HEK_{variant}$ (1199A) and **(B)** $HEK_{control}$ (CTL), $HEK_{wild\ type}$ (CGC), and $HEK_{variant}$ (CGT, TTT) cell lines. The $HEK_{control}$ (CTL) in each panel corresponds to the clone used to overexpress the corresponding transporter and transfected by the corresponding empty vector. Intensity of fluorescence is reported in arbitrary units. Results are reported as mean ± SEM (n = 9) expressed as a percentage of the CTL value (100%). Statistical analysis: 2-way ANOVA with Tukey post-hoc test, comparison between all conditions in all cell lines. Values with different letters are statistically different from each other ($P < 0.05$).

Figure 3. Impact of ABCG2 transporter on the cellular accumulation of pheophorbide a (PheA). Cell-associated fluorescence of PheA (1 µM; 5 µM) after 1 h of incubation in control conditions or in the presence of the ABCG2 inhibitor Ko143 (1 µM) in $HEK_{control}$ (CTL),

728 $HEK_{wild\ type}$ (421C) and $HEK_{variant}$ (421A). The $HEK_{control}$ (CTL) in each panel corresponds to
729 the clone used to overexpress the corresponding transporter and transfected by the
730 corresponding empty vector. Intensity of fluorescence is reported in arbitrary units. Results are
731 reported as mean ± SEM (n = 9) expressed as a percentage of the CTL value (100%). Statistical
732 analysis: 2-way ANOVA with Tukey post-hoc test, comparison between all conditions in all
733 cell lines. Values with different letters are statistically different from each other ($P < 0.05$).

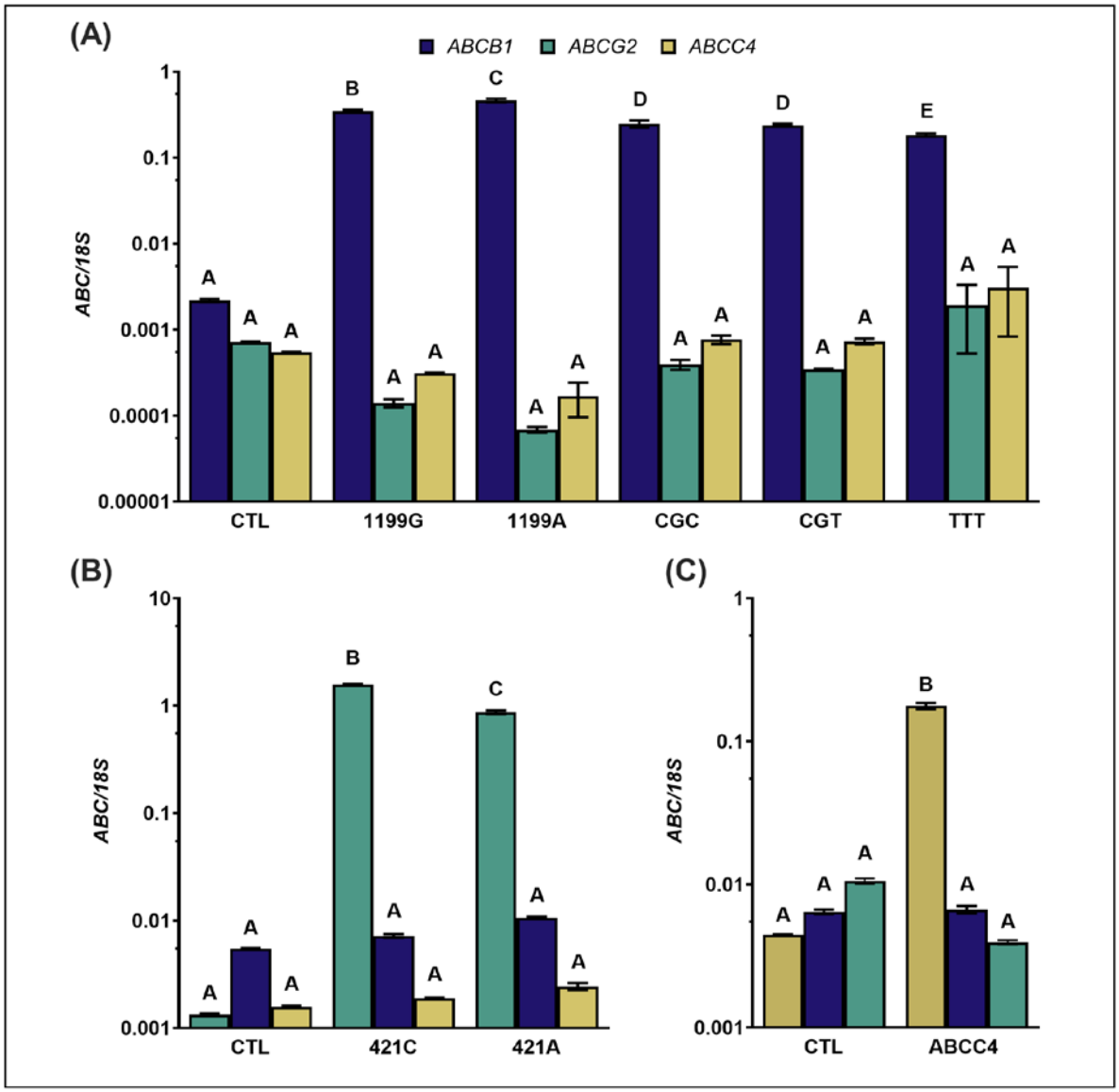
734 **Figure 4. Impact of ABCB1 and its polymorphisms on MXF and CIP cellular**
735 **accumulation.** Cellular accumulation of the fluoroquinolones (FQ) MXF and CIP (4 μg mL^{-1})
736 after 2 h of incubation in control conditions or in the presence of zosuquidar (Zo; 0.2 μM);
737 elacridar (Ela; 5 μM) ; Ko 143 (1 μM), or MK571 (25 μM) in **(A1 and A2)** $HEK_{control}$ (CTL),
738 $HEK_{wild\ type}$ (1199G), $HEK_{variant}$ (1199A), and **(B1 and B2)** $HEK_{control}$ (CTL), $HEK_{wild\ type}$
739 (CGC), $HEK_{variant}$ (CGT, TTT). The HEKcontrol (CTL) in each panel corresponds to the clone
740 used to overexpress the corresponding transporter and transfected by the corresponding empty
741 vector. Results are reported as mean ± SEM (n = 9) expressed as a percentage of the CTL value
742 (100%). Statistical analysis: 2-way ANOVA with Tukey post-hoc test, comparison between all
743 conditions in all cell lines. Values with different letters are statistically different from each other
744 ($P < 0.05$).

745 **Figure 5. Impact of ABCG2 and polymorphisms on MXF (A) and CIP (B) cellular**
746 **accumulation.** Cellular accumulation of the fluoroquinolones (FQ) MXF (**A**) and CIP (**B**) (4
747 μg mL^{-1}) after 1 h of incubation in control conditions or in the presence of Ko 143 (1 μM);
748 elacridar (Ela; 5 μM); zosuquidar (Zo; 0.2 μM) or MK571 (25 μM) in $HEK_{control}$ (CTL), $HEK_{wild\ type}$ (421C), or $HEK_{variant}$ (421A). The $HEK_{control}$ (CTL) in each panel corresponds to the clone
749
750 used to overexpress the corresponding transporter and transfected by the corresponding empty
751 vector. Results are reported as mean ± SEM (n = 9) expressed as a percentage of the CTL value

(100%). Statistical analysis: 2-way ANOVA with Tukey post-hoc test, comparison between all conditions in all cell lines. Values with different letters are statistically different from each other ($P < 0.05$).

Figure 6. Impact of ABCC4 on MXF and CIP cellular accumulation. Cellular accumulation of the fluoroquinolones (FQ) MXF (**A**) and CIP (**B**) (4 µg mL^{-1}) after 1 h of incubation in control conditions or in the presence of MK571 (10 µM, 25 µM and 50 µM), zosuquidar (Zo; 0.2 µM); elacridar (Ela; 5 µM); Ko 143 (1 µM) in $HEK_{control}$ (CTL) and HEK_{ABCC4} (ABCC4). Results are reported as mean ± SEM (n = 9) expressed as a percentage of the CTL value (100%). The $HEK_{control}$ (CTL) in each panel corresponds to the clone used to overexpress the corresponding transporter and transfected by the corresponding empty vector. Results are reported as mean ± SEM (n = 9) expressed as a percentage of the CTL value (100%). Statistical analysis: 2-way ANOVA with Tukey post-hoc test, comparison between all conditions in all cell lines. Values with different letters are statistically different from each other ($P < 0.05$).

765 **Figure 1.**



766

Figure 2.

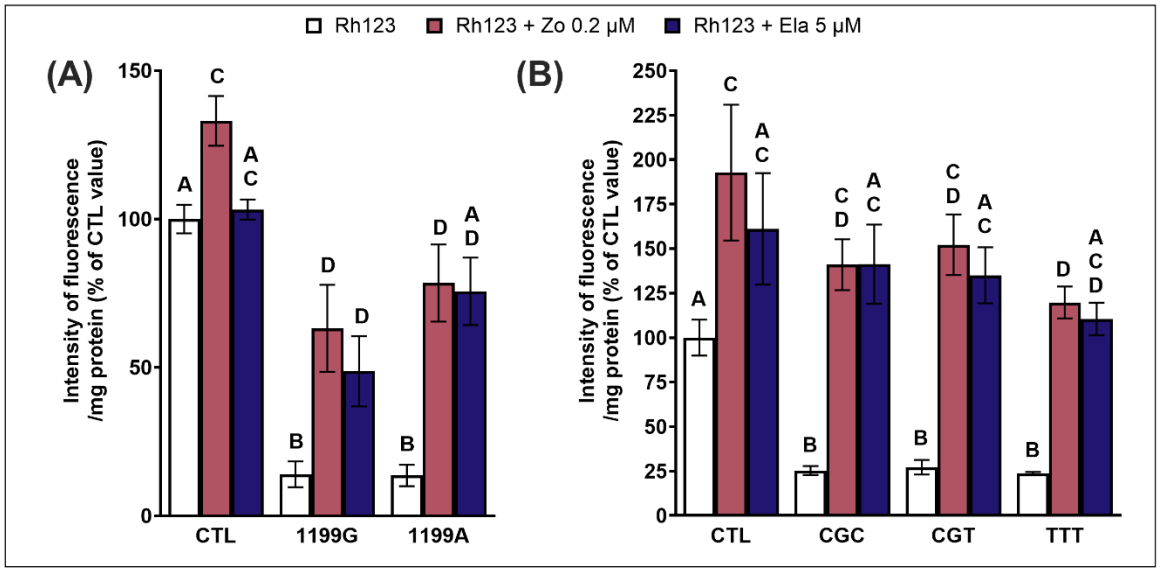
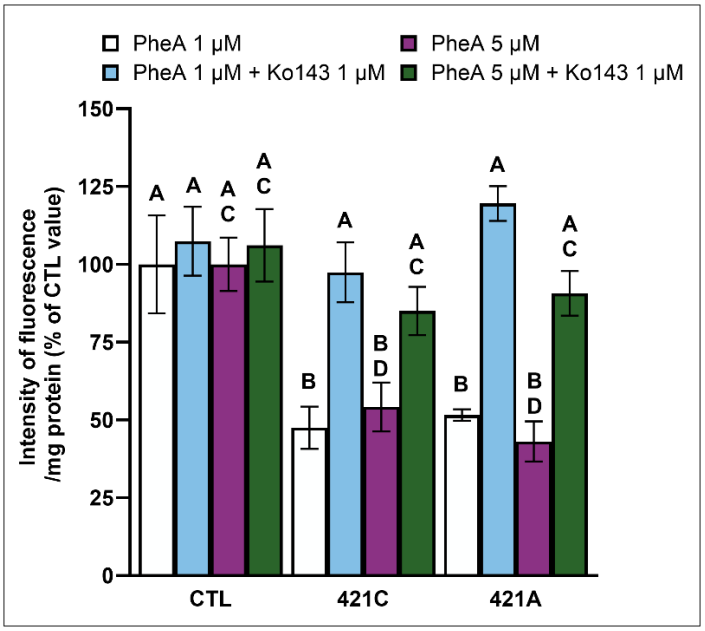
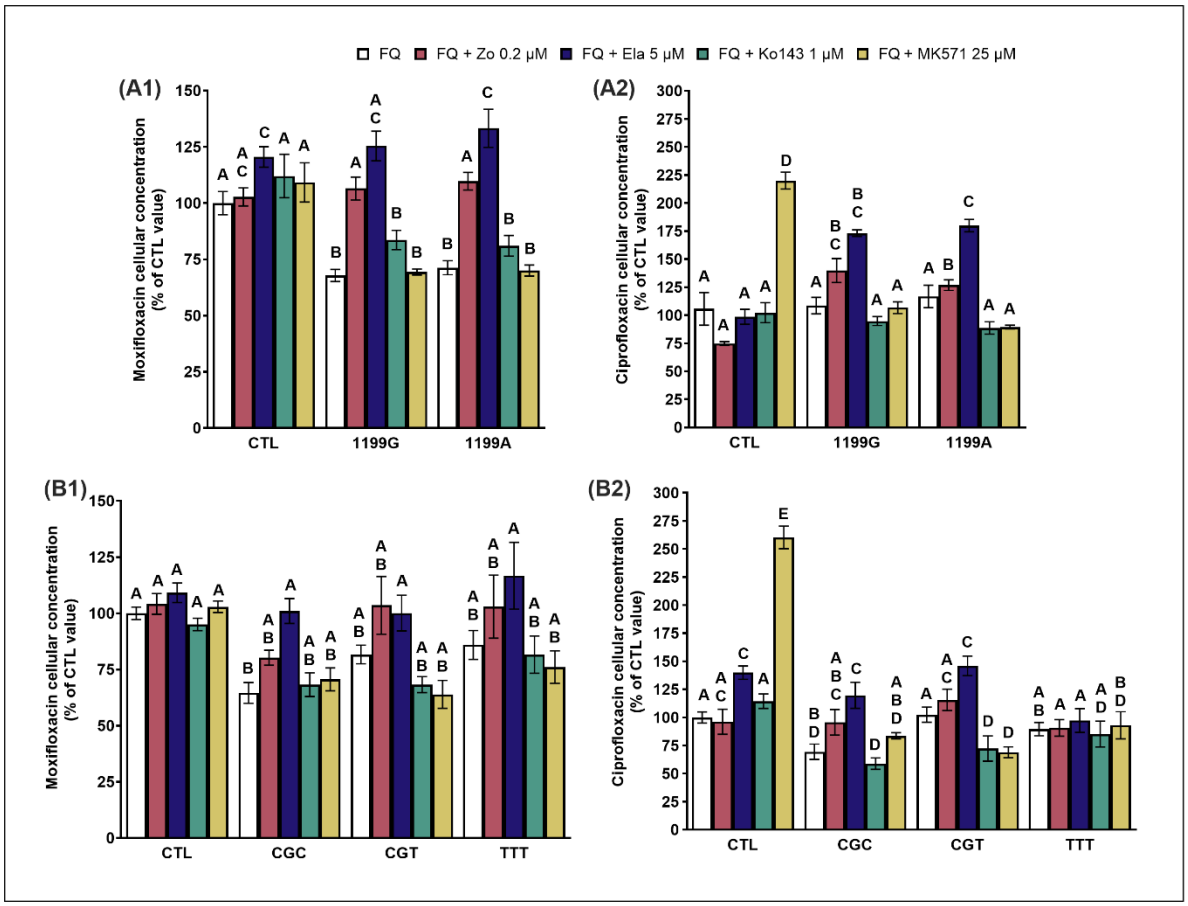

Rh123
Rh123 + Zo 0.2 µM
Rh123 + Ela 5 µM
(A)
Intensity of fluorescence /mg protein (% of CTL value)
150
100
50
0
A
C
A C
B
D
D
B
D
A D
CTL
1199G
1199A
(B)
Intensity of fluorescence /mg protein (% of CTL value)
250
225
200
175
150
125
100
75
50
25
0
A
C
A C
B
C D
A C
B
C D
A C
B
D
A C D
CTL
CGC
CGT
TTT

Figure 3.

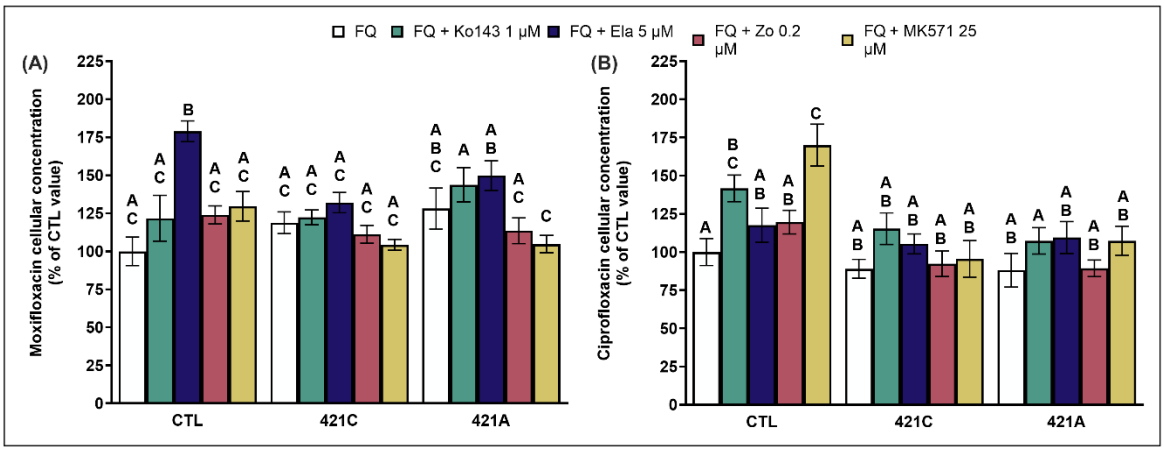

PheA 1 µM
PheA 5 µM
PheA 1 µM + Ko143 1 µM
PheA 5 µM + Ko143 1 µM
Intensity of fluorescence /mg protein (% of CTL value)
150
125
100
75
50
25
0
A
A
A C
A C
B
A
B D
A C
B
A
B D
A C
CTL
421C
421A

771 **Figure 4.**



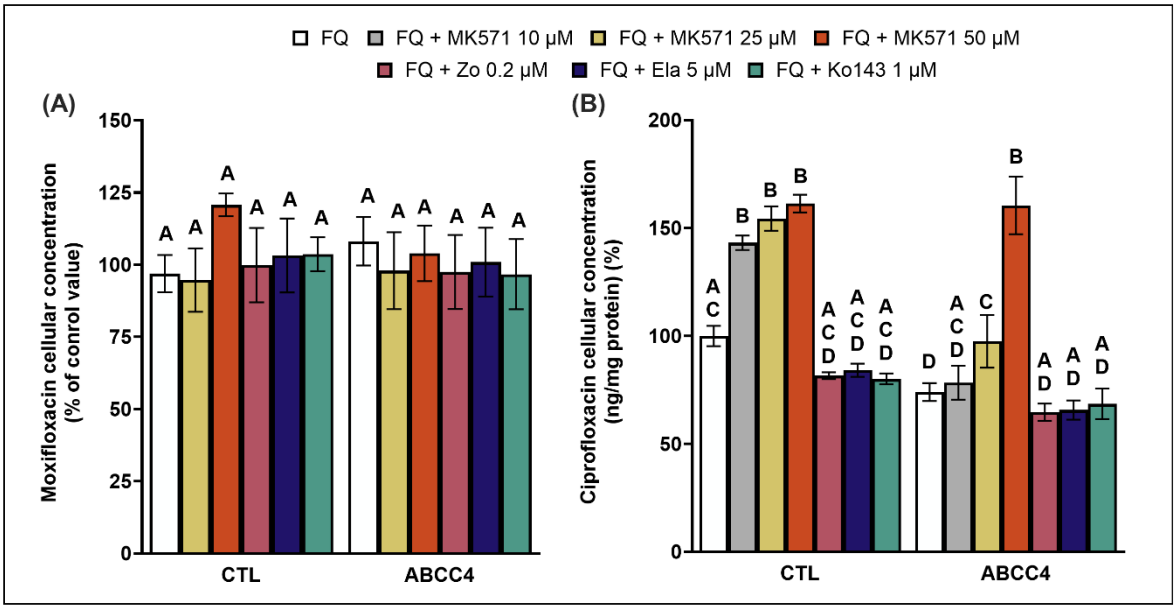
772

773 **Figure 5.**



774

Figure 6.


FQ
FQ + MK571 10 µM
FQ + MK571 25 µM
FQ + MK571 50 µM
FQ + Zo 0.2 µM
FQ + Ela 5 µM
FQ + Ko143 1 µM
(A)
Moxifloxacin cellular concentration (% of conrol value)
150
125
100
75
50
25
0
A A A A A A A A A A A A
CTL
ABCC4
(B)
Ciprofloxacin cellular concentration (ng/mg protein) (%)
200
150
100
50
0
AC B B B ACD ACD ACD D ACD C B AD AD AD
CTL
ABCC4

Supplemental Data

Figure S1. ABCB1 expression analysis by western blot. Cells transfected with empty plasmid ($HEK_{control}$ [CTL]) and cells transfected with vector cDNA encoding the ABCB1 transporter ($HEK_{wild\ type}$ [1199G], $HEK_{variant}$ [1199A]). Dilutions (from the left to the right): 1; 1/2; 1/5; 1/10.

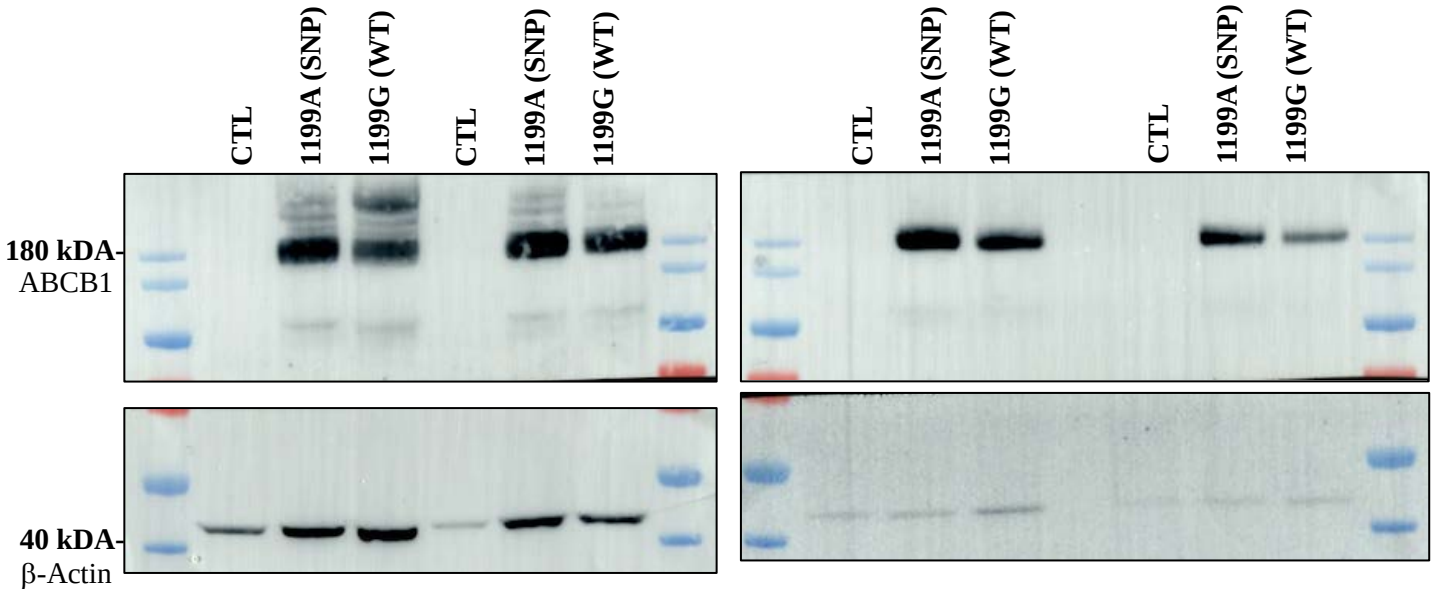


Figure S2. ABCC4 expression analysis by western blot. Cells transfected with empty plasmid ($HEK_{control}$ [CTL]) and cells transfected with vector cDNA encoding the ABCC4 transporter (HEK_{ABCC4} [ABCC4]).

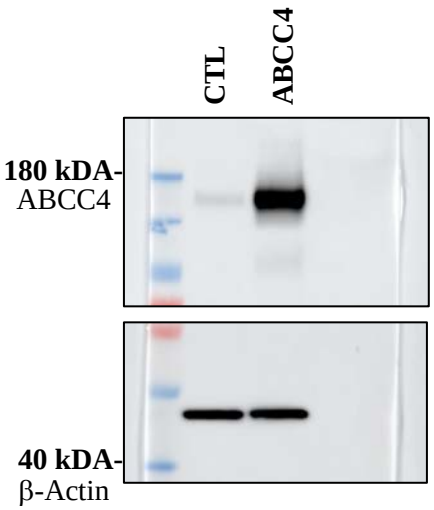


Figure S3. ABCG2 expression analysis by western blot. Cells transfected with empty plasmid ($HEK_{control}$ [CTL]) and cells transfected with vector cDNA encoding the ABCG2 transporter ($HEK_{variant}$ [421A], $HEK_{wild\ type}$ [421C]).

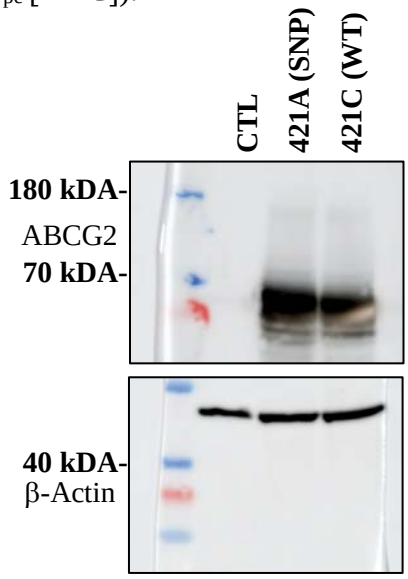
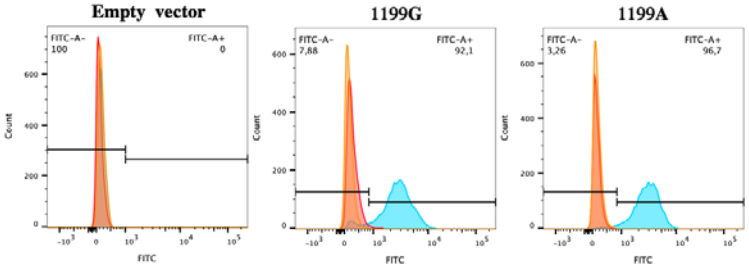
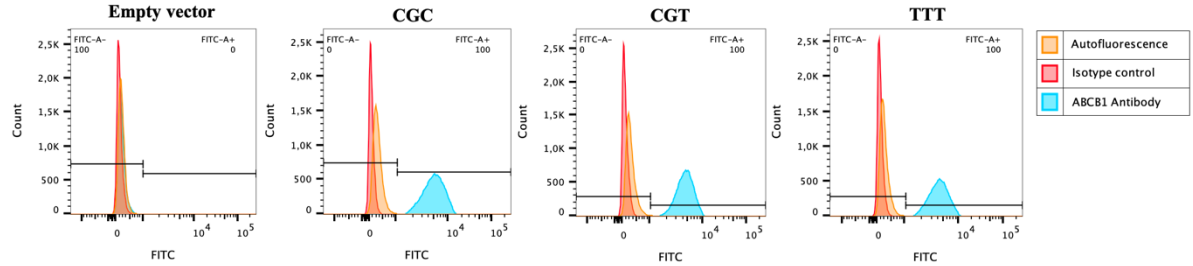


Figure S4. (A, B, C) ABCB1 and ABCG2 cell surface expression assessed by flow cytometry of HEK293 transfected cells stained with ABCB1 antibody, isotype control and no staining (autofluorescence). (A) Empty pcDNA3.1 vector, $ABCB1_{1199G}$, $ABCB1_{1199A}$. **(B)** Empty pcDNA3.1 vector, $ABCB1_{CGC}$, $ABCB1_{CGT}$, $ABCB1_{TTT}$. FITC, Fluorescein isothiocyanate. **(C)** Empty pcMV3 vector, $ABCG2_{421C}$, $ABCG2_{421A}$, PerCP (Peridinin chlorophyll)-Cy5-5-a (cyanine).

(A)



(B)



(C)

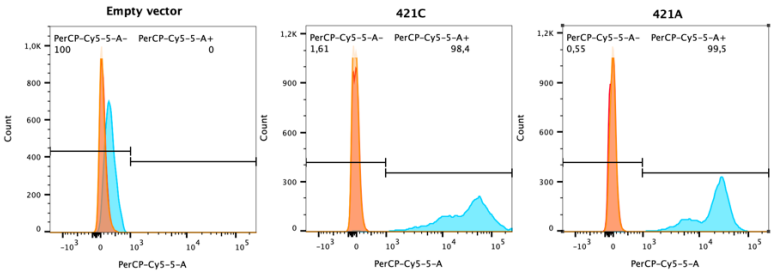


Figure S5. ABCC2 transporter RNA transcripts. ABCC2 transporter RNA expression levels normalized to the *18S* expression level (housekeeping gene) in HEKcontrol (CTL), HEK1199G>A (1199G, 1199A) and HEK1236C>T-2677G>T-3435C>T (CGC, CGT, TTT) cell lines; HEKcontrol (CTL) and HEK421C>A (421C, 421A) cell lines; HEKcontrol (CTL) and HEKABCC4 (ABCC4) cell lines.

